Systematic Electrochemical Synthesis of Reduced Forms of the α-[S2Mo18O62]4-Anion1

ARTICLE *in* INORGANIC CHEMISTRY · SEPTEMBER 1997

Impact Factor: 4.76 · DOI: 10.1021/ic970592v

Systematic Electrochemical Synthesis of Reduced Forms of the α-$[S_2Mo_{18}O_{62}]^{4-}$ Anion[1]

David M. Way,[†] John B. Cooper,[†] Maruse Sadek,[†] Truc Vu,[‡] Peter J. Mahon,[‡] Alan M. Bond,*[,‡] Robert T. C. Brownlee,[†] and Anthony G. Wedd*[,§]

Department of Chemistry, La Trobe University, Bundoora, Victoria 3083, Australia, Department of Chemistry, Monash University, Clayton, Victoria 3168, Australia, and School of Chemistry, University of Melbourne, Parkville, Victoria 3052, Australia

Received May 16, 1997[⊗]

As proton concentration increases, the first two reversible (1 e^-)-reduction processes of the anion α-$[S_2Mo_{18}O_{62}]^{4-}$ in 95/5 MeCN/H_2O convert to an overall (2 e^-)-reduction process. Half-wave potentials for reversible one-electron reduction of $[S_2Mo_{18}O_{62}]^{4-}$ itself and its two one-electron-reduced forms $[S_2Mo_{18}O_{62}]^{5-}$ and $[HS_2Mo_{18}O_{64}]^{4-}$ were estimated by voltammetry to be 0.12, −0.13, and 0.35 V, respectively, versus the ferrocenium/ferrocene couple. Simulation of cyclic voltammograms provided estimates of association constants of 1.4, 1.6×10^8, and 10^2 M^{-1} for protonation of the respective products of the reductions, $[S_2Mo_{18}O_{62}]^{5-}$, $[S_2Mo_{18}O_{62}]^{6-}$, and $[HS_2Mo_{18}O_{62}]^{5-}$. Equilibrium constants for disproportionation of the (1 e^-)-reduced species were derived. Rates of the electron transfer and protonation processes are very fast relative to the voltammetric time scale. Consideration of the equilibrium constants, plus information obtained from acid titrations monitored by steady state voltammetry, helped define conditions for the isolation of salts of the (1 e^-)-, (2 e^-)-, (2 e^-, 1 H^+)-, (2 e^-, 2 H^+)-, (4 e^-, 2 H^+)- and (4 e^-, 4 H^+)-reduced derivatives of the $[S_2Mo_{18}O_{62}]^{4-}$ anion. Anions at the (6 e^-)- and (8 e^-)-reduced levels undergo spontaneous oxidation in the acid solutions and could not be isolated experimentally. The present work shows that directed synthesis of reduced species in different protonation states is possible for these complex systems if adequate voltammetric data are available.

Introduction

Polyoxometalate anions which feature MO_6 octahedra with a single terminal oxo ligand are reducible to intensely colored compounds known as "poly blues".[2,3] These are class II mixed-valence compounds[4] in which thermally mobile electrons transfer between octahedra.[2,3,5−18] Rich redox and photochemical properties follow from this feature.[19,20]

The present work examines the reductive chemistry of $[S_2Mo_{18}O_{62}]^{4-}$, whose α-isomer exhibits the so-called Dawson structure (see structure **I** in Chart 1).[21,22] This chemistry has been evolving steadily.[17,23−29] Eight reversible one-electron reductions, falling into four pairs, are seen in very dry acetonitrile.[29] These coalesce into four overall two-electron reductions upon the addition of acid. A further 10 electrons can be added reversibly under acid conditions, resulting in an 18-electron-reduced species, stable on the voltammetric time scale.[29] This corresponds to formal reduction of all 18 Mo(VI) centers in α-$[S_2Mo_{18}O_{62}]^{4-}$ to Mo(V).

Salts of the 1e^-- and 2e^--reduced products of $[S_2Mo_{18}O_{62}]^{4-}$ have been isolated experimentally, and a (4e^-, 3H^+)-reduced form has been characterized structurally.[17,28] The structure of the oxidized tungstate $[P_2W_{18}O_{62}]^{6-}$ is close to the D_{3h} representation of structure **I**.[21] In the molybdenum analog, alternating molybdenum atoms in the two Mo_6 equatorial belts are displaced so that the belts are puckered, reducing the point symmetry to D_3.[30] This gives rise to chirality and even optical activity.[31,32] The distortion is present but much less developed in $[S_2Mo_{18}O_{62}]^{4-}$ and nearly disappears in the (4e^-, 3H^+)-

* Corresponding authors. E-mail address: a.bond@sci.monash.edu.au; t.wedd@chemistry.unimelb.edu.au.
† La Trobe University.
‡ Monash University.
§ University of Melbourne.
⊗ Abstract published in *Advance ACS Abstracts,* August 1, 1997.

(1) Abbreviations: b, broad; Bu, *n*-C_4H_9; *d*, diameter; $E_{1/2}$, reversible half-wave potential; *F*, Faraday's constant; *K*, equilibrium constant; k_b, backward rate constant; k_f, forward rate constant; Hex, *n*-C_6H_{13}; Fc, Fe(η^5-C_5H_5)$_2$; *n*, number of electrons transferred per mole; Pr, *n*-C_3H_7; sh, shoulder; *T*, temperature; *v*, scan rate.

(2) Pope, M. T. *Heteropoly and Isopoly Oxometalates*; Springer-Verlag: Berlin, 1983; pp 101−117.
(3) Pope, M. T.; Müller, A. *Angew. Chem., Int. Ed. Engl.* **1991**, *30*, 34.
(4) Robin, M. B.; Day, P. *Adv. Inorg. Chem. Radiochem.* **1967**, *10*, 247.
(5) Prados, R. A.; Pope, M. T. *Inorg. Chem.* **1976**, *15*, 2547.
(6) Che, M.; Fournier, M.; Launay, J. P. *J. Chem. Phys.* **1979**, *71*, 1954.
(7) Launay, J. P.; Fournier, M.; Sanchez, C.; Livage, J.; Pope, M. T. *Inorg. Nucl. Chem. Lett.* **1980**, *16*, 257.
(8) Pope, M. T. In *Mixed Valence Compounds*; Brown, D. B., Ed.; Reidel Publishing: Dordrecht, The Netherlands, 1980; p 365.
(9) Sanchez, C.; Livage, J.; Launay, J. P.; Fournier, M.; Jeannin, Y. *J. Am. Chem. Soc.* **1982**, *104*, 3194.
(10) Sanchez, C.; Livage, J.; Doppelt, P.; Chauveau, F.; Lefebvre, J. *J. Chem. Soc., Dalton Trans.* **1982**, 2439.
(11) Sanchez, C.; Livage, J.; Launay, J. P.; Fournier, M. *J. Am. Chem. Soc.* **1983**, *105*, 6817.
(12) Harmalker, S. P.; Leparulo, M. A.; Pope, M. T. *J. Am. Chem. Soc.* **1983**, *105*, 4286.
(13) Kozik, M.; Hammer, C. F.; Baker, L. C. W. *J. Am. Chem. Soc.* **1986**, *108*, 2748.
(14) Kozik, M.; Hammer, C. F.; Baker, L. C. W. *J. Am. Chem. Soc.* **1986**, *108*, 7627 and references therein.
(15) Piepgrass, K.; Barrows, J. N.; Pope, M. T. *J. Chem. Soc., Chem. Commun.* **1989**, 10.
(16) Casan-Pastor, N.; Baker, L. C. W. *J. Am. Chem. Soc.* **1992**, *114*, 10384.
(17) Cooper, J. B.; Way, D. M.; Bond, A. M.; Wedd, A. G. *Inorg. Chem.* **1993**, *32*, 2416.
(18) Duncan, D. C.; Hill, C. L. *Inorg. Chem.* **1996**, *35*, 5828.
(19) Hill, C. L.; Prosser-McCartha, C. *Coord. Chem. Rev.* **1995**, *143*, 407.
(20) Bond, A. M.; Way, D. M.; Wedd, A. G.; Compton, R. G.; Booth, J.; Eklund, J. C. *Inorg. Chem.* **1995**, *34*, 3378.
(21) Dawson, B. *Acta Crystallogr.* **1953**, *6*, 113.
(22) Hori, T.; Tamada, O.; Himeno, S. *J. Chem. Soc., Dalton Trans.* **1989**, 1491.
(23) Hori, T.; Himeno, S. *Chem. Lett.* **1987**, 53.
(24) Cartié, B. *J. Chem. Res., Synop.* **1988**, 290.
(25) Himeno, S.; Hori, T.; Saito, A. *Bull. Chem. Soc. Jpn.* **1989**, *62*, 2184.
(26) Cooper, J. B.; Bond, A. M.; Oldham, K. B. *J. Electroanal. Chem. Interfacial Electrochem.* **1992**, *331*, 877.
(27) Himeno, S.; Osakai, T.; Saito, A.; Maeda, K.; Hori, T. *J. Electroanal. Chem. Interfacial Electrochem.* **1992**, *337*, 371.
(28) Neier, R.; Trojanowski, C.; Mattes, R. *J. Chem. Soc., Dalton Trans.* **1995**, 2521.
(29) Way, D. M.; Bond, A. M.; Wedd, A. G. *Inorg. Chem.* **1997**, *36*, 2826.
(30) Strandberg, R. *Acta. Chem. Scand., Ser. A.* **1975**, *29*, 350, 359.
(31) Pope, M. T. *Inorg. Chem.* **1976**, *15*, 2008.
(32) Garvey, J. F.; Pope, M. T. *Inorg. Chem.* **1978**, *17*, 1115.

S0020-1669(97)00592-2 CCC: $14.00

Chart 1. Polyhedral Representation of α-$[S_2Mo_{18}O_{62}]^{4-}$ (D_{3h} Point Symmetry)

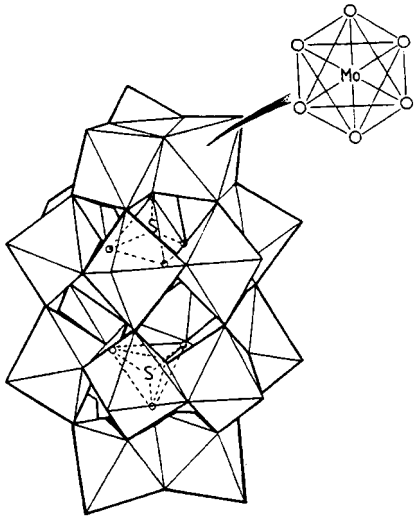

I

reduced form.[22,28] The mean deviation of the molybdenum atoms from the two least-squares planes defined by the two Mo_6 belts decreases from 0.18 Å in the oxidized form to 0.007 Å in the reduced form. The oxo ligands bridging the Mo_3 caps to the Mo_6 equatorial belts of structure **I** appear to be the sites of protonation.

The first quantitative investigation of reduction of a polyoxometalate anion was performed in 1920.[33] The direct influence of protonic equilibria on the redox chemistry was apparent then, and detailed investigations followed.[34−36] The present work shows that simulation of voltammograms as a function of proton concentration allows quantitative estimation of equilibrium constants for proton association and disproportionation of reduced polyoxo anions. When coupled with a knowledge of the dependence of half-wave potentials on proton concentration in strongly acid media, this information directs synthesis of reduced derivatives of $[S_2Mo_{18}O_{62}]^{4-}$ in different protonation states.

Experimental Section

Reagents. In addition to those reagents described previously,[17] acetonitrile (chromatographic AR HPLC grade, Mallinckrodt) used for voltammetry was purified further.[37] Voltammetric glassware was cleaned in detergent, heated in nitric acid (16 M), and rinsed with deionized water before drying at 100 °C.

Instrumentation. IR spectra were acquired in the diffuse reflectance mode on 1−2% mixtures of sample in KBr on a Perkin-Elmer 1720X Fourier transform spectrometer equipped with an Epson PC AX2 computer. Electronic spectra were obtained on Cary 17 and Shimadzu UV-240 spectrometers. ^{1}H and ^{17}O NMR spectra were recorded on a Bruker AM-300 spectrometer equipped with a 5 mm multinuclear probe.

Voltammetric instrumentation, cells, and methods were as described previously.[17] All potentials are quoted relative to the ferrocenium/ferrocene couple, Fc^+/Fc, unless otherwise stated. The working electrodes of choice were glassy carbon disks (d = 1.0 or 3.0 mm) and a platinum microelectrode ($d = 100$ μm). Before each experiment, the glassy carbon electrode was polished on a polishing pad (LECO Inc.) using 1.0 and 0.25 mm Metadi diamond polishing compound (Buehler Ltd.). The Pt microelectrode was polished with 0.05 μm deagglomerated alumina (Cypress). Each electrode were rinsed with deionized water, polished again on a polishing pad with water only, rinsed, and dried with hot air. Bulk electrolysis and coulometry at platinum mesh electrodes were carried out as described previously.[17]

Simulation of Cyclic Voltammograms. The simulation package DIGISIM V 2.0 (Bioanalytical Systems, West Lafayette, IN) is described in detail in ref 37. It was run on a 150 MHz Pentium PC. Each simulation required about 5 s.

Synthesis. Microanalysis was performed by the Analytische Laboratorien, Gummersbach, Germany. The Hex_4N^+ and Bu_4N^+ salts were synthesized as described previously.[17]

$(Bu_4N)_5[S_2Mo_{18}O_{62}]$. Electrosynthesis of this green salt from $(Bu_4N)_4[S_2Mo_{18}O_{62}]$ in MeCN was reported in ref 17. Use of 2 mM solutions in CH_2Cl_2 (100 mM Bu_4NClO_4) is more efficient because analytically pure product precipitates progressively during electrolysis. This prevents contamination of the salt with the products of its H^+-induced disproportionation.

$(Pr_4N)_6[S_2Mo_{18}O_{62}]$ and $(Bu_4N)_5[HS_2Mo_{18}O_{62}]$. A solution of $(Hex_4N)_4[S_2Mo_{18}O_{62}]$ (2.4 mM) in MeCN (60 mL; 240 mM Bu_4NClO_4) was reduced at −0.45 V. Pr_4NBr (0.25 g) was added to the deep-blue solution, and the mixture was covered with perforated plastic film and stored at −5 °C. After 1 week, blue crystals were isolated, washed with EtOH, and dried under vacuum. Anal. Calcd for $C_{72}H_{168}Mo_{18}N_6O_{62}S_2$: C, 22.15; H, 4.31; N, 2.15; S, 1.64. Found: C, 22,31; H, 4.22; N, 2.13; S, 1.69. If no Pr_4NBr is added and the solution is stored at 4 °C, then the protonated ($2e^-$, H^+) product $(Bu_4N)_5[HS_2Mo_{18}O_{62}]$ crystallizes. Anal. Calcd for $C_{80}H_{181}Mo_{18}N_5O_{62}S_2$: C, 24.03; H, 4.53; N, 1.75. Found: C, 23.92; H, 4.51; N, 1.78.

$(Pr_4N)_5[HS_2Mo_{18}O_{62}]$. A solution of $(Hex_4N)_4[S_2Mo_{18}O_{62}]$ (5.0 mM), $HClO_4$ (20 mM), and Bu_4NClO_4 (200 mM) in 95/5 MeCN/H_2O was reduced at 0.15 V. Voltammetric monitoring of the dark blue-green solution with the Pt microelectrode confirmed a two-electron reduction (i.e., the point of zero current was at the plateau between the first and second waves). Pr_4NBr (0.072 g; 0.27 mmol) was added and the beaker covered with perforated plastic film. Storage at 4 °C produced needlelike dark blue-green crystals after 1 h. These were isolated, washed with EtOH, and dried under vacuum (yield: 0.103 g; 56%). Anal. Calcd for $C_{60}H_{141}Mo_{18}N_5O_{62}S_2$: C, 19.38; H, 3.77; N, 1.88; S, 1.72. Found: C, 20.92; H, 3.87; N, 2.33; S, 1.55. Inclusion of up to three molecules of MeCN of crystallization improves agreement with experiment. Calcd for $C_{66}H_{150}Mo_{18}N_8O_{62}S_2$: C, 20.64; H, 3.91; N, 2.92; S, 1.67. Et_4N^+ and Bu_4N^+ salts can be synthesized in a similar manner.

$(Hex_4N)_4[H_2S_2Mo_{18}O_{62}]$. A solution of $(Hex_4N)_4[S_2Mo_{18}O_{62}]$ (5.0 mM) and $HClO_4$ (200 mM) in 95/5 MeCN/H_2O was reduced at 0.14 V. Voltammetric monitoring confirmed a two-electron reduction. Hex_4NBr (0.63 g; 1.5 mmol) was added and the beaker covered with perforated plastic film. Storage at 4 °C for 4 weeks produced blue crystals, which were isolated, washed with EtOH, and dried under vacuum (yield: 0.17 g; 79%). The mother liquor yielded further product upon continued slow evaporation at 4 °C. Anal. Calcd for $C_{96}H_{210}Mo_{18}N_4O_{62}S_2$: C, 27.41; H, 5.00; N, 1.33; S, 1.53. Found: C, 26.93; H, 4.89; N, 1.26, S, 1.52. Pr_4N^+ and Bu_4N^+ salts can be synthesized in a similar manner.

$(Pr_4N)_6[H_2S_2Mo_{18}O_{62}]$. This salt was obtained as blue crystals using a procedure equivalent to that for $(Pr_4N)_5[HS_2Mo_{18}O_{62}]$ except that the electrolysis potential was set at 0 V. Voltammetric monitoring of the blue solution confirmed a four-electron reduction. Anal. Calcd for $C_{72}H_{170}Mo_{18}N_6O_{62}S_2$: C, 22.14; H, 4.36; S, 1.64. Found: C, 23.45; H, 4.50; S, 1.59. Inclusion of three molecules of MeCN of crystallization improves agreement with experiment. Calcd for $C_{78}H_{179}Mo_{18}N_9O_{62}S_2$: C, 23.27; H, 4.48; S, 1.59. A Bu_4N^+ salt can be synthesized in a similar manner.

$(Hex_4N)_4[H_4S_2Mo_{18}O_{62}]$. This salt was obtained as deep blue crystals using a procedure equivalent to that for $(Hex_4N)_4[H_2S_2Mo_{18}O_{62}]$ except that the electrolysis potential was set at 0.09 V. Voltammetric monitoring of the deep blue solution confirmed a four-electron reduction. Anal. Calcd for $C_{96}H_{212}Mo_{18}N_4O_{62}S_2$: C, 27.41; H, 5.09; N, 1.33; S, 1.52. Found: C, 26.97; H, 4.90; N, 1.27; S, 1.48. Pr_4N^+ and Bu_4N^+ salts can be synthesized in a similar manner.

(33) Wu, H. *J. Biol. Chem.* **1920**, *43*, 189.
(34) Contant, R.; Fruchart, J.-M. *Rev. Chim. Miner.* **1974**, *11*, 123.
(35) Pope, M. T.; Papaconstantinou, E. *Inorg. Chem.* **1967**, *6*, 1147 and references therein.
(36) Papaconstantinou, E.; Pope, M. T. *Inorg. Chem.* **1967**, *6*, 1152.
(37) Kiesele, H. *Anal. Chem.* **1980**, *52*, 2230.
(38) Rudolph, M.; Reddy, D. P.; Feldberg, S. W. *Anal. Chem.* **1994**, *66*, 589A.

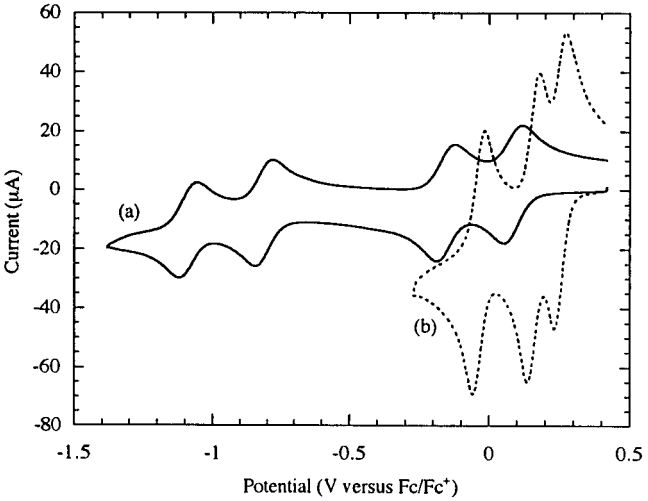

Figure 1. Cyclic voltammograms of solutions of α-$[S_2Mo_{18}O_{62}]^{4-}$ (1 mM; Bu_4NClO_4, 100 mM) at a glassy carbon disk electrode (d = 3.0 mm): (a) MeCN; (b) 95/5 MeCN/H_2O ($HClO_4$, 3 M). Scan rate = 500 mV s^{-1}.

Results and Discussion

Voltammetry as a Function of Acid Concentration. In dry MeCN, reduction of α-$[S_2Mo_{18}O_{62}]^{4-}$ occurs in eight one-electron processes, falling into four pairs, in the potential range +0.1 to −2.7 V versus the Fc^+/Fc couple.[29] Figure 1a illustrates the first four processes. The first two remain clearly defined in unbuffered 95/5 MeCN/H_2O (Figure 2: no acid), implying that reaction with available protons is not significant on the voltammetric time scale in this mixed-solvent system. Addition of acid allows observation of eight chemically reversible processes in the range 0 to −1.5 V in which 2, 2, 2, 2, 4, 4, 2, and 8 electrons, respectively, are transferred.[29] Figure 1b shows the first three two-electron reduction waves, seen in the presence of excess $HClO_4$. $E_{1/2}$ values estimated from the voltammograms are listed in Table 1.

The interesting region with respect to acid concentration in unbuffered media occurs when the concentrations of acid and polyoxo anion are similar. Upon titration of $HClO_4$ into a 1 mM solution of $[S_2Mo_{18}O_{62}]^{4-}$ in 95/5 MeCN/H_2O, the first two one-electron waves convert progressively to the first two-electron wave (Figure 2). The processes responsible for the one-electron waves are written explicitly in eq 1. The voltam-

$$[S_2Mo_{18}O_{62}]^{4-} \overset{e^-}{\rightleftharpoons} [S_2Mo_{18}O_{62}]^{5-} \overset{e^-}{\rightleftharpoons} [S_2Mo_{18}O_{62}]^{6-} \quad (1)$$

mograms of Figure 2 were simulated assuming Scheme 1, which incorporates eq 1 and protonation equilibria between the (1 e^-)- and (2 e^-)-reduced species. Scheme 1 evolved from the following considerations:

(i) The oxidized anion $[S_2Mo_{18}O_{62}]^{4-}$ was assumed to be unprotonated, consistent with the general observation that oxidized polyoxo anions are very weak bases.[39] Experimentally, vis−UV and electrospray mass spectra are independent of $[H^+]$ up to 100 mM.

(ii) Initial estimates of the two $E_{1/2}$ values of eq 1 were made voltammetrically (cf. Table 1).

(iii) A value of 6.4×10^{-6} cm^2 s^{-1} was taken for the diffusion coefficient of $[S_2Mo_{18}O_{62}]^{4-}$ in MeCN at 25 °C.[28] It was assumed to be the same for each anion under the conditions of the present work. The equivalent parameter for H^+ is unknown in MeCN/H_2O solutions. Best fits were obtained with a value of 1.8×10^{-5} cm^2 s^{-1}.

(39) Barcza, L.; Pope, M. T. *J. Phys. Chem.* **1973**, *77*, 1795.

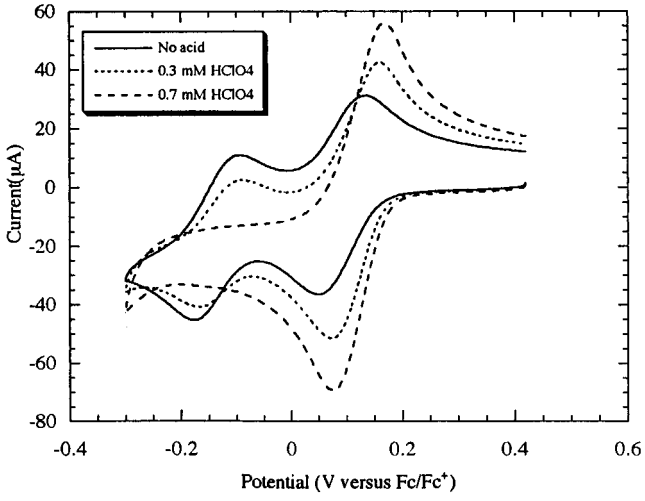

Figure 2. Cyclic voltammograms in 95/5 MeCN/H_2O as a function of $HClO_4$ concentration. Other experimental conditions are as in Figure 1.

Table 1. $E_{1/2}$ Values for Reduction of $(Hex_4N)_4[S_2Mo_{18}O_{62}]$ (2.0 mM) in MeCN Solutions[a]

	MeCN[c] $[Bu_4NClO_4]$ (M)		95/5 MeCN/H_2O $[HClO_4]$ (M)		
n[b]	0.1[c]	0.2[d]	0[c]	10^{-3} [d]	10^{-2} [e]
1	0.12	0.10	0.18		
2	−0.12	−0.13	−0.05	0.19	0.31
3	−0.78	−0.80	−0.72		
4	−1.05	−1.07	−1.08	0.09	0.22
5		−1.67			
6		−1.92		−0.11	0.03
7		−2.36[f]			
8		−2.72[f]		−0.41	−0.28

[a] Potentials versus Fc^+/Fc. [b] Total number of electrons added at this potential. [c] Estimated by cyclic voltammetry (glassy carbon disk; d = 3.0 mm; v = 100 mV s^{-1}). [d] As for footnote *c* but with v = 10 V s^{-1}. [e] As for footnote *d* except that Bu_4NClO_4 electrolyte was absent. [f] −30° C.

Scheme 1

$$[S_2Mo_{18}O_{62}]^{4-} \overset{e^-}{\rightleftharpoons} [S_2Mo_{18}O_{62}]^{5-} \overset{e^-}{\rightleftharpoons} [S_2Mo_{18}O_{62}]^{6-}$$

$$\downarrow\uparrow H^+ \qquad \downarrow\uparrow H^+$$

$$[HS_2Mo_{18}O_{62}]^{4-} \overset{e^-}{\rightleftharpoons} [HS_2Mo_{18}O_{62}]^{5-}$$

$$\downarrow\uparrow H^+$$

$$[H_2S_2Mo_{18}O_{62}]^{4-}$$

(iv) The forward rate constants k_f of the three protonation equilibria were assumed to be large (10^{10} M^{-1} s^{-1}). The backward rate constants k_b were allowed to vary.

Comparisons of experiment and theory are made in Figure 3. Agreement is excellent at the six H^+ concentrations examined in the range 0−0.7 mM and for scan rates of 20, 50, 100, and 500 mV s^{-1}. This success validates the assumptions that the heterogeneous and homogeneous rates of the redox and protonation processes are very fast relative to the voltammetric time scale and that the redox processes are diffusion controlled under this range of conditions. It is clear that while the observed waves differ in relative current intensity as $[H^+]$ varies (Figure 2), this does not imply irreversibility. Parameters $E_{1/2}$ and $K = k_f/k_b$ are listed in Table 2.

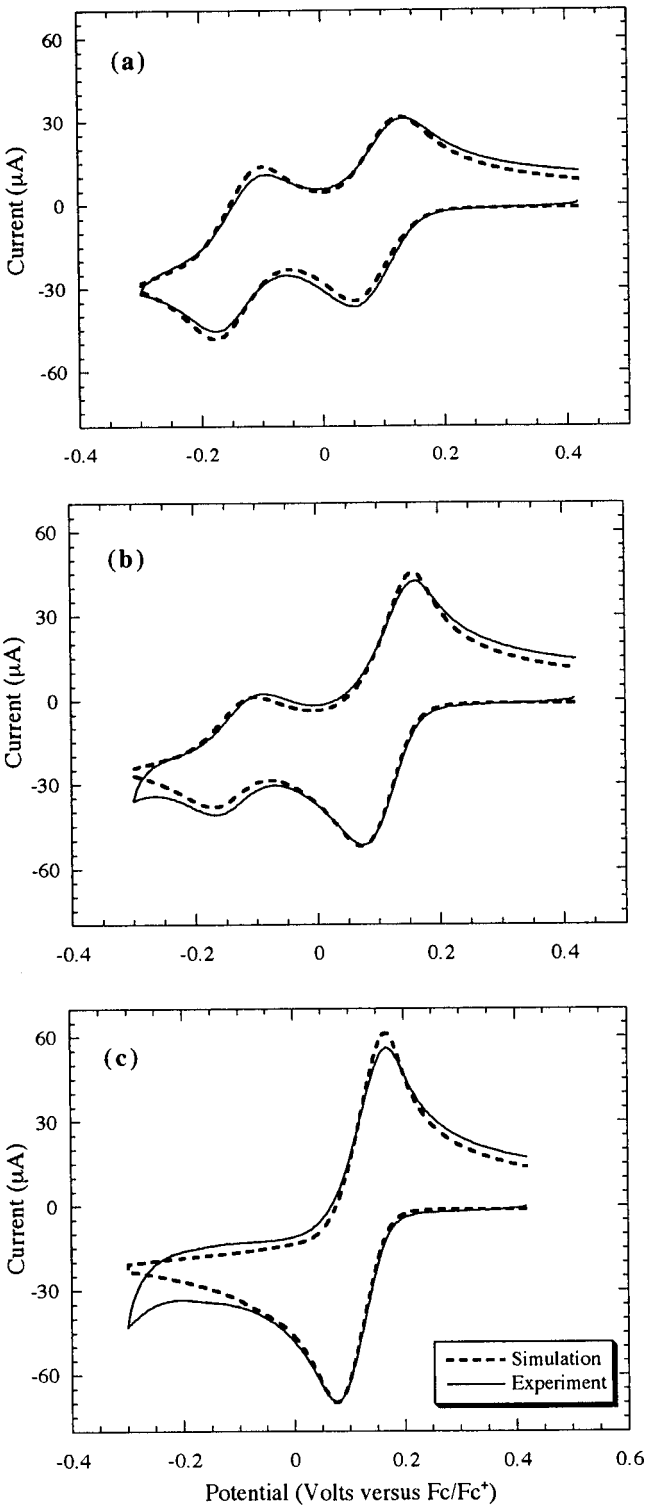

Figure 3. Simulation of cyclic voltammograms. [$HClO_4$], mM: (a) 0; (b) 0.3; (c) 0.7. Other experimental conditions are as in Figure 2.

The results confirm that the two one-electron reversible processes of eq 1 occur in 95/5 MeCN/H_2O in the absence of acid. However, in the presence of acid, the (1 e^-)-reduction product $[S_2Mo_{18}O_{62}]^{5-}$ protonates rapidly and reversibly to form an equilibrium with $[HS_2Mo_{18}O_{62}]^{4-}$ (Table 2):

$$[S_2Mo_{18}O_{62}]^{5-} \overset{H^+}{\rightleftharpoons} [HS_2Mo_{18}O_{62}]^{4-} \qquad (2)$$

$$K_2 = 1.4\ M^{-1}$$

The more basic (2 e^-)-reduction product $[S_2Mo_{18}O_{62}]^{6-}$ forms an equilibrium favoring $[H_2S_2Mo_{18}O_{62}]^{4-}$ over $[HS_2Mo_{18}O_{62}]^{5-}$:

Table 2. Parameters for Simulation of Cyclic Voltammograms[a,b]

charge transfer reactions	$E_{1/2}$, V
$[S_2Mo_{18}O_{62}]^{4-} \overset{e^-}{\rightleftharpoons} [S_2Mo_{18}O_{62}]^{5-}$	0.10
$[S_2Mo_{18}O_{62}]^{5-} \overset{e^-}{\rightleftharpoons} [S_2Mo_{18}O_{62}]^{6-}$	−0.13
$[HS_2Mo_{18}O_{62}]^{4-} \overset{e^-}{\rightleftharpoons} [HS_2Mo_{18}O_{62}]^{5-}$	0.35

protonation reactions	K, M^{-1}
$[S_2Mo_{18}O_{62}]^{5-} \overset{H^+}{\rightleftharpoons} [HS_2Mo_{18}O_{62}]^{4-}$	1.4
$[S_2Mo_{18}O_{62}]^{6-} \overset{H^+}{\rightleftharpoons} [HS_2Mo_{18}O_{62}]^{5-}$	1.6×10^8
$[HS_2Mo_{18}O_{62}]^{5-} \overset{H^+}{\rightleftharpoons} [H_2S_2Mo_{18}O_{62}]^{4-}$	10^2

[a] See Figure 3. [b] Derived diffusion coefficients: 1.8×10^{-5} $cm^2\ s^{-1}$ for the proton and 6.4×10^{-6} $cm^2\ s^{-1}$ for all polyoxo anions.

$$[S_2Mo_{18}O_{62}]^{6-} \xrightarrow{H^+} [HS_2Mo_{18}O_{62}]^{5-} \qquad (3)$$

$$K_3 = 1.6 \times 10^8\ M^{-1}$$

$$[HS_2Mo_{18}O_{62}]^{5-} \overset{H^+}{\rightleftharpoons} [HS_2Mo_{18}O_{62}]^{4-} \qquad (4)$$

$$K_4 = 10^2\ M^{-1}$$

As shown previously, the (1 e^-)-reduction product is essentially stable to disproportionation under aprotic conditions:[17]

$$2[S_2Mo_{18}O_{62}]^{5-} \rightleftharpoons [S_2Mo_{18}O_{62}]^{4-} + [S_2Mo_{18}O_{62}]^{6-} \qquad (5)$$

$$K_5 = 10^{-4}$$

However, the $E_{1/2}$ value for reduction of $[S_2Mo_{18}O_{62}]^{5-}$ is much more negative than that for its protonated form $[HS_2Mo_{18}O_{62}]^{4-}$ (−0.13 versus 0.35 V; Table 2), and so, in the presence of acid, the system is unstable to disproportionations 6 and 7.

$$[S_2Mo_{18}O_{62}]^{5-} + [HS_2Mo_{18}O_{62}]^{4-} \rightleftharpoons [S_2Mo_{18}O_{62}]^{4-} + [HS_2Mo_{18}O_{62}]^{5-} \qquad (6)$$

$$K_6 = 1.6 \times 10^4$$

$$[S_2Mo_{18}O_{62}]^{5-} + [HS_2Mo_{18}O_{62}]^{4-} + H^+ \rightleftharpoons [S_2Mo_{18}O_{62}]^{4-} + [H_2S_2Mo_{18}O_{62}]^{4-} \qquad (7)$$

$$K_7 = 1.6 \times 10^4\ M^{-1}$$

The final state of protonation of the two-electron-reduction product of eqs 6 and 7 will depend on $[H^+]$ due to the influence of equilibrium 4.

In principle, the coalescence of all the (1 e^-)-reduction processes into (2 e^-) processes could be simulated. However, a number of complications arise, such as the influence of redox cross-reactions, and so simulation of the initial processes only was attempted at this stage.

Nernstian Behavior. For high acid concentrations, it can be assumed that, during the course of the voltammetry, $[H^+]$ remains constant at its bulk solution value at the electrode surface. This simplifying feature means that an analytical solution is available to interpret the dependence of $E_{1/2}$ on $[H^+]$. The overall equation for an electrode process for the reduction of an (m e^-, y H^+)-reduced species is thermodynamically equivalent to

$$\alpha\text{-}[H_yS_2Mo_{18}O_{62}]^{(4-y+m)-} + xH^+ + ne^- \rightleftharpoons \alpha\text{-}[H_{x+y}S_2Mo_{18}O_{62}]^{(4-y-x+m+n)-} \qquad (8)$$

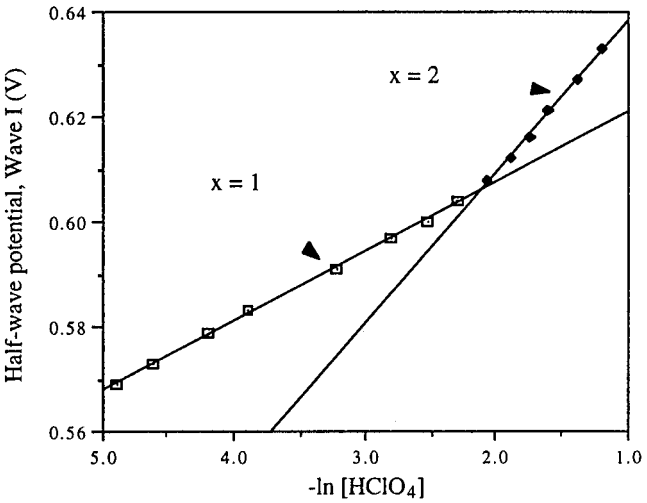

Figure 4. Dependence of $E_{1/2}$ for the first two-electron-reduction process on $[HClO_4]$ in 95/5 MeCN/H_2O. Experimental conditions are as in Figure 2, except for $[Bu_4NClO_4]$, 10 mM.

The Nernst equation indicates that a plot of $E_{1/2}$ versus $-\ln [H^+]$ will have a slope of $(x - y)RT/nF$. As discussed above, the number of protons y associated with the oxidized form $[S_2Mo_{18}O_{62}]^{4-}$ can be safely assumed to be zero. Since $n = 2$ for the first reduction process seen at $[H^+] > 0.7$ mM (Figures 1 and 2), it follows that the slope will be $xRT/2F$.

Employing steady state voltammetry at the Pt microelectrode,[29] we estimated $E_{1/2}$ values for the first three two-electron processes (Figure 1b) as a function of $[HClO_4]$ in the range 7.5−300 mM. Figure 4 shows a plot of $E_{1/2}$ for the first process versus $-\ln [H^+]$ for a solution of $(Hex_4N)_4[S_2Mo_{18}O_{62}]$ (0.4 mM) in 95/5 MeCN/H_2O containing Bu_4NClO_4 (10 mM). There is a linear dependence with $x = 1$ for $[HClO_4] < 100$ mM but with $x = 2$ for $[HClO_4] > 120$ mM, consistent with stabilization of different protonation states for the two-electron-reduced product in the two ranges:

$$[S_2Mo_{18}O_{62}]^{4-} + H^+ + 2\ e^- \rightleftharpoons [HS_2Mo_{18}O_{62}]^{5-} \quad (9)$$

$$[S_2Mo_{18}O_{62}]^{4-} + 2H^+ + 2\ e^- \rightleftharpoons [H_2S_2Mo_{18}O_{62}]^{4-} \quad (10)$$

Equivalent behavior is seen in Figure S1 (Supporting Information) for formation of the four- and six-electron-reduced products:

$$[HS_2Mo_{18}O_{62}]^{5-} + H^+ + 2\ e^- \rightleftharpoons [H_2S_2Mo_{18}O_{62}]^{6-} \quad (11)$$

$$[H_2S_2Mo_{18}O_{62}]^{4-} + 2H^+ + 2\ e^- \rightleftharpoons [H_4S_2Mo_{18}O_{62}]^{4-} \quad (12)$$

$$[H_2S_2Mo_{18}O_{62}]^{6-} + H^+ + 2\ e^- \rightleftharpoons [H_3S_2Mo_{18}O_{62}]^{7-} \quad (13)$$

$$[H_4S_2Mo_{18}O_{62}]^{4-} + 2H^+ + 2\ e^- \rightleftharpoons [H_6S_2Mo_{18}O_{62}]^{4-} \quad (14)$$

The sharp breakpoints in the titrations, coupled with the $E_{1/2}$ values of the individual steps, imply that the reduced forms are far more basic than the oxidized forms from which they are derived. All of the species listed in eqs 9−14 are in equilibrium with other protonated forms. The analysis only identifies the major species present at a given proton concentration.

Figure S2 (Supporting Information) shows analogous data for $[HClO_4]$, 10−100 mM, with the Bu_4NClO_4 concentration increased by a factor of 10 to 100 mM. Under these conditions, two protons are consumed per two electrons transferred at all proton concentrations (eqs 10, 12, and 14). The different behavior may be a consequence of ionic strength, particularly the effect of ion pairing. The latter may be significant when an anion of overall charge 4− is dissolved in such a mixed-solvent system with different electrolyte concentrations. Himeno also reports $x = 2$ at similar ionic strengths.[25]

Synthesis. The (1 e^-)- and (2 e^-)-reduced species, $[S_2Mo_{18}O_{62}]^{5-}$ and $[S_2Mo_{18}O_{62}]^{6-}$, are predicted to be accessible synthetically in the absence of acid (Tables 1 and 2; Figure 1) and, indeed, have been isolated experimentally.[17] Equations 3, 4, 6, and 7 indicate that the (2 e^-, 1 H^+)- and (2 e^-, 2 H^+)-reduced species, $[HS_2Mo_{18}O_{62}]^{5-}$ and $[H_2S_2Mo_{18}O_{62}]^{4-}$, should be stabilized at low and high $[H^+]$, respectively. In contrast, the (1 e^-, 1 H^+)-reduced anion $[HS_2Mo_{18}O_{62}]^{4-}$ will not be accessible (eqs 2 and 6). These conclusions are augmented by Figures 4, S1, and S2, which provide possible conditions of $HClO_4$ concentration and ionic strength for the generation, by controlled-potential electrolysis, of anions of differing redox and protonation states. In practice, definition of the optimum conditions for isolation of pure materials was guided by the above conclusions and by considerations such as the rate of electrolysis, relative solubilities, and precipitation rates.

Controlled-potential electrolysis, coupled with coulometry and monitoring with steady state voltammetry, confirmed that each

Table 3. Spectroscopic Data

	electronic			infrared, cm^{-1} [b]				^1H NMR[c]	
anion[a]	solvent	λ_{max} (nm)	$10^{-3}\epsilon$, M^{-1} cm^{-1}	$\nu_{as}(SO_4)$	$\nu_s(SO_4)$	ν(Mo═O)	ν_{as}(MoOMo)	δ, ppm	rel intens
$[S_2Mo_{18}O_{62}]^{4-}$	MeCN	310 sh	34	1169	1067	965, 953 sh	890 sh, 828		
	MeCN						798		
$[S_2Mo_{18}O_{62}]^{5-}$ (1e⁻)	MeCN	295 sh	38	1169	1069	957, 946 sh	873 sh, 834		
		840 sh	2.5				784,756 sh		
		1040	4.3						
$[S_2Mo_{18}O_{62}]^{6-}$ (2e⁻)		290 sh	37	1168 sh	1065	950, 942 sh	870 sh, 825		
		645 sh	8.3	1162			778, 760 sh		
		825	11						
$[HS_2Mo_{18}O_{62}]^{5-}$	(95/5) MeCN/H_2O +	300 sh	27	1162	1066	957, 947 sh	864 sh, 829	4.3	1 ± 0.2
(2e⁻, 1H^+)	1 mM $HClO_4$	575 sh	3.3				783, 764 sh		
		755	8.2						
$[H_2S_2Mo_{18}O_{62}]^{4-}$	(95/5) MeCN/H_2O +	300 sh	42	1166 sh	1067	966, 952	819 b, 730 sh	5.3	2 ± 0.2
(2e⁻, 2H^+)	10 mM $HClO_4$	601 sh	5.9	1160					
		761	13						
$[H_2S_2Mo_{18}O_{62}]^{6-}$	(95/5) MeCN/H_2O +			1160	1066, 1059 sh	959, 945 sh	828 sh, 790		
(4e⁻, 2H^+)	1 mM $HClO_4$						747, 739		
$[H_4S_2Mo_{18}O_{62}]^{4-}$	(95/5) MeCN/H_2O +	298 sh	42	1160	1074	969, 950	838, 816		
(4e⁻, 4H^+)	10 M $HClO_4$	687	24	1153 sh	1057		748, 729		
		730 sh	23						

[a] The numbers of electrons and protons added to the $[S_2Mo_{18}O_{62}]^{4-}$ ion are indicated in parentheses. [b] 1−2% sample in KBr; reflectance mode. [c] CD_3CN; 22 °C; intensity estimated relative to the resonance of the cation α protons.

of the first two (2 e^-) processes observed with $[HClO_4] = 20$ and 200 mM is chemically reversible: reoxidation leads to quantitative regeneration of the original species. Salts of the two- and four-electron-reduction products are obtained from MeCN/$HClO_4$(aq) solutions in protonation states which vary with the proton concentration. The (2 e^-, 1 H^+) and (4 e^-, 2 H^+) products, $[HS_2Mo_{18}O_{62}]^{5-}$ and $[H_2S_2Mo_{18}O_{62}]^{6-}$, were obtained when $[HClO_4] = 20$ mM while the (2 e^-, 2 H^+) and (4 e^-, 4 H^+) products, $[H_2S_2Mo_{18}O_{62}]^{4-}$ and $[H_4S_2Mo_{18}O_{62}]^{4-}$, were obtained when $[HClO_4] = 200$ mM. A (6 e^-)-reduced form is also produced efficiently in solution, and reoxidation produces the oxidized form quantitatively. However, upon standing, the reduced solution oxidizes spontaneously (reduction of H^+?), preventing isolation of salts. Similar observations hold for more highly reduced solutions.

The salts isolated are characterized in Table 3, and full details of their preparation are provided in the Experimental Section. Purity and stoichiometry were determined by microanalysis and by monitoring the point of zero current in steady state voltammograms of the salts dissolved in the media from which they were isolated (Figure 5; cf. ref 17). The latter technique allows, for example, the Hex_4N^+ salts of the oxidized anion $[S_2Mo_{18}O_{62}]^{4-}$, the (2 e^-, 2 H^+) product $[H_2S_2Mo_{18}O_{62}]^{4-}$, and the (4 e^-, 4 H^+) product $[H_4S_2Mo_{18}O_{62}]^{4-}$ to be distinguished. They differ in composition by only two and four hydrogen atoms in a molar mass of 4204 Da. The positions of the zero current in Figure 5 confirm that $(Hex_4N)_4[H_2S_2Mo_{18}O_{62}]$ is two-electron-reduced and that $(Hex_4N)_4[H_4S_2Mo_{18}O_{62}]$ is four-electron-reduced. Singlet resonances of relative intensities 1 and 2 were observed in the ^1H NMR spectra of the two-electron-reduced anions $[HS_2Mo_{18}O_{62}]^{5-}$ and $[H_2S_2Mo_{18}O_{62}]^{4-}$ in dry CD_3CN (Table 3).

The addition of acid to the (1 e^-)-reduced anion $[S_2Mo_{18}O_{62}]^{5-}$ causes disproportionation (eqs 6 and 7; ref 17). The oxidation level of the (2 e^-)-reduced anion $[S_2Mo_{18}O_{62}]^{6-}$ is confirmed by its steady state voltammogram (Figure 6a). Addition of acid leads to the (2 e^-, 2 H^+) behavior characteristic of $[S_2Mo_{18}O_{62}]^{4-}$ in acidified MeCN (Table 1). The position of zero current is at the plateau between the first two two-electron waves (Figure 6b) and shows that $[S_2Mo_{18}O_{62}]^{6-}$ is protonated (via eqs 3 and 4) but does not disproportionate.

There are intense absorptions around 300 nm in the oxidized anion $[S_2Mo_{18}O_{62}]^{4-}$, characteristic of O → W charge transfer transitions. In addition, each of the reduced anions exhibits broad absorption in the visible and near-infrared regions, characteristic of intervalence $W^V \rightarrow W^{VI}$ charge transfer (Table 3).[2] In common with other systems, the extinction coefficients for the long-wavelength band maxima are approximately proportional to the number of electrons added. Note that more than one protonation state may contribute to the observed spectra.

A number of factors could lower the effective point symmetry of α-$[S_2Mo_{18}O_{62}]^{4-}$ (structure **I**) upon reduction, including isomerization and anisotropic electron and proton distributions. Isomerization of α to *β* forms is proposed to occur upon reduction of α-$[X_2Mo_{18}O_{62}]^{6-}$ (X = P, As) in aqueous solution.[34] Infrared spectra of oxidized Keggin and Dawson isomers, particularly the frequencies of the *ν*(MoOMo) modes involving corner-sharing octahedra, are sensitive to the orientation of the trimetallic capping units.[40,41] Data on the present systems are provided in Table 3. The similarity of the spectra of α-$[S_2Mo_{18}O_{62}]^{4-}$ and its (2 e^-, *x* H^+; *x* = 0−2) derivatives above 900 cm^{-1} in the solid state is consistent with these all

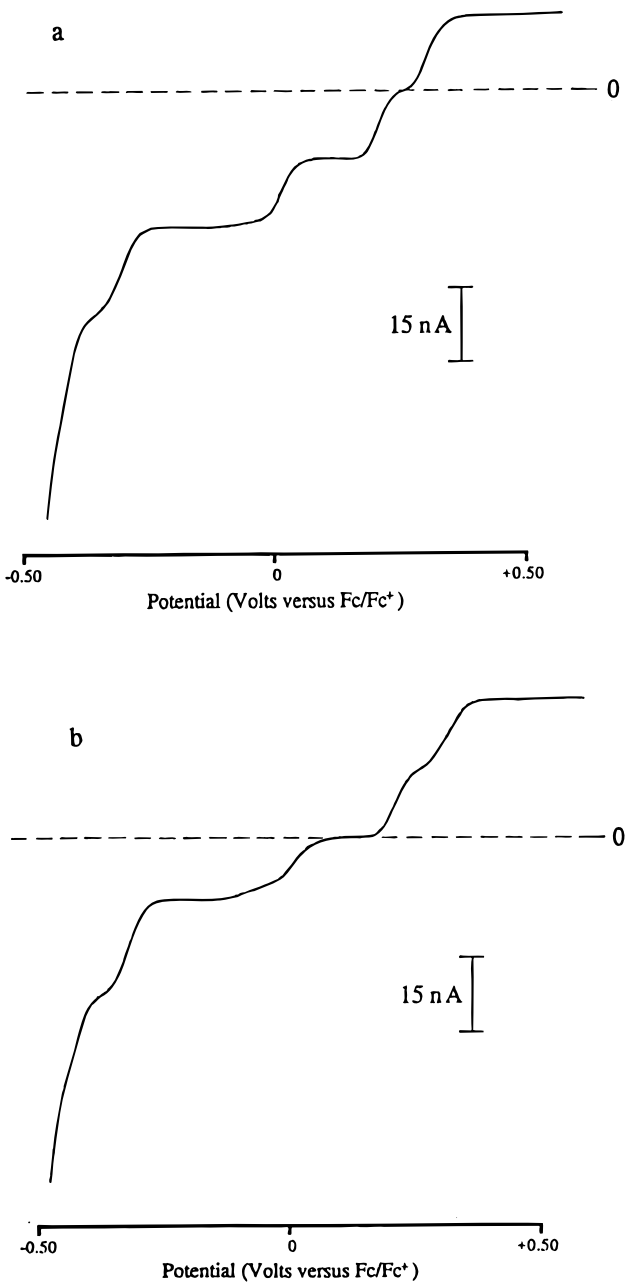

Figure 5. Near steady state voltammograms of 1 mM solutions of Hex_4N^+ salts at a Pt microelectrode ($d = 100$ *μ*m) in 95/5 MeCN/H_2O (Bu_4NClO_4, 200 mM; $HClO_4$, 100 mM): (a) $[H_2S_2Mo_{18}O_{62}]^{4-}$; (b) $[H_4S_2Mo_{18}O_{62}]^{4-}$.

being α isomers. Pronounced splitting of *ν*(SO_4) and *ν*-(MoOMo) modes is seen in the (4 e^-, *x* H^+; *x* = 2, 4) forms and is similar to that reported for the structurally-characterized (4 e^-, 3 H^+) derivative α-$[H_3S_2Mo_{18}O_{62}]^{5-}$.[28] Unfortunately, none of the crystalline salts isolated in the present work diffracted X-rays to high resolution.

^{17}O NMR spectra of the reduced forms in solution are complicated by protonic equilibria (cf. eqs 2−4 and 6,7).[42] However, the spectra of the oxidized anion $[S_2Mo_{18}O_{62}]^{4-}$ and the (2 e^-)-reduced products $[H_xS_2Mo_{18}O_{62}]^{(6-x)-}$ (*x* = 0−2) in 95/5 MeCN/H_2O ($[HClO_4] = 0-20$ mM) show two resonances, separated by 23 ± 3 ppm, in the chemical shift range 900−950 ppm relative to $H_2{}^{17}O$. These might be assigned to the two inequivalent Mo═O sites present in the α isomer (structure

(40) Thouvenot, R.; Fournier, M.; Franck, R.; Rocchiccioli-Deltcheff, C. *Inorg. Chem.* **1984**, *23*, 598.
(41) Contant, R.; Thouvenot, R. *Inorg. Chim. Acta* **1993**, *212*, 41.
(42) Way, D. M. Ph.D. Thesis, La Trobe University, 1996.
(43) Klemperer, W. G. *Angew. Chem., Int. Ed. Engl.* **1978**, *17*, 246.
(44) Pope, M. T. In *Progress in Inorganic Chemistry*; Lippard, S. J., Ed.; John Wiley & Sons: New York, 1991; Vol. 39, p 181.

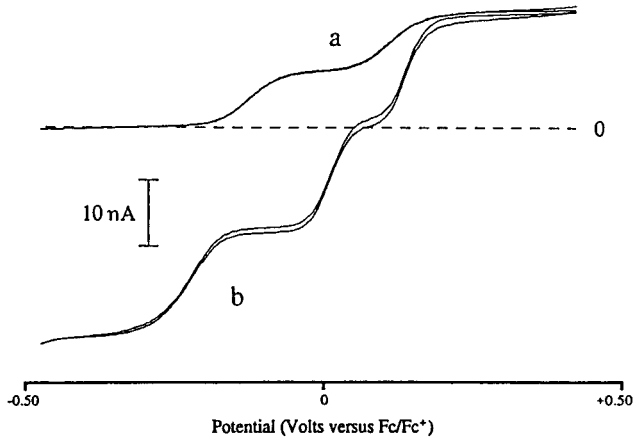

Figure 6. Near steady state voltammograms of $(Pr_4N)_6[S_2Mo_{18}O_{62}]$ (2.3 mM): (a) in MeCN (230 mM Bu_4NClO_4); (b) after addition of 3.8 mM $HClO_4$.

I).[43,44] Detailed analysis of the NMR properties of these reduced species will be reported in due course.

Conclusions. The present work shows that simulation of cyclic voltammograms as a function of proton concentration allows, for the first time, quantitative estimation of the protonation and disproportionation constants of reduced polyoxo anions. When these were combined with titration data monitored by steady state voltammetry, conditions were defined for the experimental isolation of salts of the (1 e^-)-, (2 e^-)-, (2 e^-, 1 H^+)-, (2 e^-, 2 H^+)-, (4 e^-, 2 H^+)-, and (4 e^-, 4 H^+)-reduced derivatives. Different conditions may provide different protonation states. For example, the following reaction led to the Bu_4N^+ salt of the (4 e^-, 3 H^+) derivative[28]

$$[S_2Mo_{18}O_{62}]^{4-} + 2PPh_3 + 2H_2O \xrightarrow{\Delta,\ MeCN} [H_3S_2Mo_{18}O_{62}]^{5-} + 2OPPh_3 + H^+ \quad (15)$$

This reaction was not under synthetic control. The present work shows that directed synthesis of reduced species in different protonation states is possible for these complex systems if adequate voltammetric data are available.

Acknowledgment. A.G.W. and A.M.B. thank the Australian Research Council for support via Grant A29531579.

Supporting Information Available: Figures S1 and S2, showing plots of the dependence of $E_{1/2}$ upon $[HClO_4]$ (2 pages). Ordering information is given on any current masthead page.

IC970592V